



Short communication

Synthesis of high-voltage spinel cathode material with tunable particle size and improved temperature durability for lithium ion battery

Yi-Chun Jin^a, Ming-I Lu^b, Tsung-Hsiung Wang^b, Chang-Rung Yang^b, Jenq-Gong Duh^{a,*}^a Department of Materials Science and Engineering, National Tsing Hua University, Taiwan^b Material and Chemical Research Lab., Industrial Technology Research Institute, Chutung, Hsinchu 31040, Taiwan

HIGHLIGHTS

- The polymer-mediating method is employed in powder fabrication.
- The particle size of spinel is tunable from nanometer to micrometer.
- Nanometric spinels perform a high rate capability due to fast Li-intercalations.
- Micrometric spinels demonstrate an improved cycling stability at high temperature.

ARTICLE INFO

Article history:

Received 19 December 2013

Received in revised form

3 March 2014

Accepted 19 March 2014

Available online 26 March 2014

Keywords:

Polymer-mediating

Particle size

Temperature durability

Spinel cathode material

Lithium ion battery

ABSTRACT

In this study, a one-pot method of polymer-mediating process is proposed to synthesize high voltage spinels ($\text{LiNi}_{1/2}\text{Mn}_{3/2}\text{O}_4$) with tunable particle size and high-crystallization. The primary particle size can be controlled from nanometer to micrometer via changing different type of polymer additives. Relationships between particle sizes and electrochemical performances at wide temperature ranges ($-20\text{ }^{\circ}\text{C}$ – $55\text{ }^{\circ}\text{C}$) are investigated. Nano-sized spinel delivers a good rate capability and higher capacitance at both room and low temperatures, while the micro-sized spinel performs better in capacity retention, especially at elevated temperature. The correlations among the particle size, temperature durability and cycling stability are demonstrated. Besides, the influence of polymer-mediation on the morphology transformation of spinel is also probed and discussed.

© 2014 Elsevier B.V. All rights reserved.

1. Introduction

Lithium nickel manganese spinel ($\text{LiNi}_{1/2}\text{Mn}_{3/2}\text{O}_4$) is recently of considerable interest for promising cathode material in lithium ion battery owing to its ultimate high working potential ($\sim 4.7\text{ V}$) and great power capability [1–3]. Other advantages, such as low cost, abundant supply, environmental friendliness and safety characteristics of $\text{LiNi}_{1/2}\text{Mn}_{3/2}\text{O}_4$ are also compared to the commercial LiCoO_2 cathode.

The fabrication of spinel with ternary or quaternary lithium transition-metal oxides requires high temperature treatments [4,5]. These conditions, such as solid-state reaction [6,7], increase

the crystal growth rate and hinder the obtainment of nanometric particles. Thus, the alternative of using a low thermal treatment, such as sol–gel [8] or emulsion drying [9], was applied. However, these methods usually produce materials of low crystallinity that are frequently accompanied by organic impurities coming from an organic matrix commonly used in some stage of the synthesis procedure. Other methods, such as composite carbonate process [10], molten salt [11], ultrasonic spray pyrolysis method [12] and co-precipitation [13,14] were also demonstrated to prepare spinel materials. Yet, drawbacks detract from these methods of both complex reaction and poor particle uniformity.

Besides, these studies reported only fabrication result or room temperature performance of $\text{LiNi}_{1/2}\text{Mn}_{3/2}\text{O}_4$ powders, no detailed synthetic approach relevant to particle size and cycling durability at a wide temperature range ($55\text{ }^{\circ}\text{C}$ to $-20\text{ }^{\circ}\text{C}$) was provided. Moreover, there was no single one-pot method to synthesize $\text{LiNi}_{1/2}\text{Mn}_{3/2}\text{O}_4$.

* Corresponding author. #101 Sec. II, Kuang-Fu Rd., Hsinchu 30013, Taiwan. Tel./fax: +886 3 5712686.

E-mail address: jgd@mx.nthu.edu.tw (J.-G. Duh).

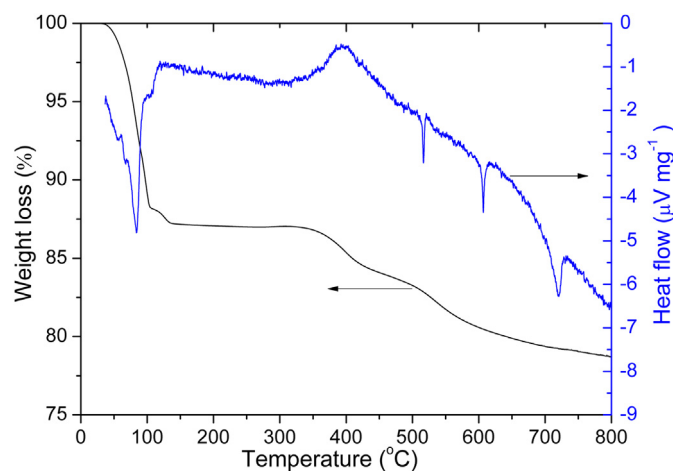


Fig. 1. The TG-DSC measurement of Li–Ni–Mn–O precursors pre-heated at 400 °C for 3 h.

O_4 with high-crystallinity and controllable particle sizes at a fixed temperature.

Therefore, in this study, effective strategy for modifying the textural properties of $\text{LiNi}_{1/2}\text{Mn}_{3/2}\text{O}_4$ is proposed via using various polymer additives. A simple direct process fabricates high-crystallized spinel compound with tunable particle sizes from nanometers to micrometers at a fixed calcination temperature around 700 °C. The electrochemical performances on temperature durability correlated with size discrepancy are also discussed.

2. Experimental procedure

Hydrate metal chlorides ($\text{LiCl} \cdot \text{H}_2\text{O}$, $\text{MnCl}_2 \cdot 6\text{H}_2\text{O}$, and $\text{NiCl}_2 \cdot 6\text{H}_2\text{O}$) were used as the cationic sources, and oxalic acid as the reagent acid mixed with different functional polymers (polyethylene glycol, polyacrylic acid and polyimide). Firstly, metal chlorides of the stoichiometric composition ratio (Li: Ni: Mn = 2: 1: 3) were dissolved in the aqueous oxalic acid, and a green solution was then produced by heating at 90 °C for 30 min. In the meantime, appropriate amount (5–10 wt.% of the precursor route) of polymer was added drop wisely with stirring for forming the three dimensional polymeric matrix. The resulting product was pre-heated at 150 °C for 1 h and then calcined at 700 °C for 10 h in an air atmosphere.

The microstructural and electrochemical properties of synthesized compounds were characterized by several techniques. Powder X-ray diffractometer (Rigaku-6000) was applied for phase identifications with a Cu-K α radiation. Field emission scanning electron microscope (JSM-7300, JOEL) was used for morphological observations. Thermogravimetric analyzer (TGA-7, Perkin Elmer) was carried out under air flow of 20 mL min^{-1} with a heating rate of

$10 \text{ }^\circ\text{C min}^{-1}$ for investigation of calcination process. The electrochemical cells consisted of Spinel-based composite ($\text{LiNi}_{1/2}\text{Mn}_{3/2}\text{O}_4$; active carbon: polyvinylidene fluoride = 0.8: 0.13 :0.07 in wt.%) as the positive electrode, Li-metal as the negative electrode, and an electrolyte of 1 M LiPO_4 in a 1:1 volumetric mixture of ethylene carbonate and dimethyl carbonate. All cells were assembled in an argon-filled dry box with controlled water and oxygen concentrations below 0.01 ppm.

Arbin battery testing system (BT-2000) was employed to test the 2032 type coin cells with Celgard 2400 membrane as the cell separator. Charge–discharge retention tests were performed at a constant current density ranging from 0.9 to 0.7 mA cm^{-2} with the cut-off voltage between 3.5 and 5 V. The specific capacity values were calculated from the value of the current, the mass of active material in the cathode, and the elapsed time. Impedance spectra were measured by impedance analyzer (Model 263A, EG&G). The frequency was varied from 10 mHz to 100 kHz with an AC oscillation of 30 mV. While measuring the impedance spectra, a DC bias voltage was matched to the open-circuit voltage (OCV) of the cell.

3. Results and discussion

The preparation of a homogeneous polymeric precursor is the most crucial step in the synthesis procedure of polymer-mediating process [15]. Several main steps are proposed here for fabricating spinel compound in this study. Firstly, the metathesis reacted between metal chelates and reagent acid at ambient temperature. Secondly, low temperature pyrolysis associated with dehydration of functional polymer below 200 °C. Afterward, the degradation of polymers took place below 450 °C, accompanying with the great release of carbon dioxide. Finally, the formation of spinel phase was accomplished after annealing at 700 °C for 10 h Fig. 1 displays the TG measurement of Li–Ni–Mn compound heated from 25 to 850 °C, whereas the precursor sintered at 400 °C for 3 h. The result shows that the formation of spinel phase is around 500–700 °C, corresponding to the gradually stopping of weight losses.

Fig. 2(a–d) represents the FE-SEM images of as-synthesized $\text{LiNi}_{1/2}\text{Mn}_{3/2}\text{O}_4$ powders. The significant size divergence was observed after pre-mediating different polymers. The primary particle size of pristine spinels (without any polymer mediation) is around 0.5–1 μm . After mediating of PAA or PEG, the particle size showed a noticeable shrinkage from sub-microns down to nanometers (100–300 nm).

The previous results strongly support the assumption that the chain structured polymer forms a barrier that hinders particle growth [16,17]. Polymeric surfactants are known to adsorb to the surfaces of growing particles and create a shield against van der Waals interactions between them. Consequently, the particle aggregation and agglomeration can be greatly inhibited and resulted in nanometric powders. Fig. 3(a) illustrates the mixture of metal

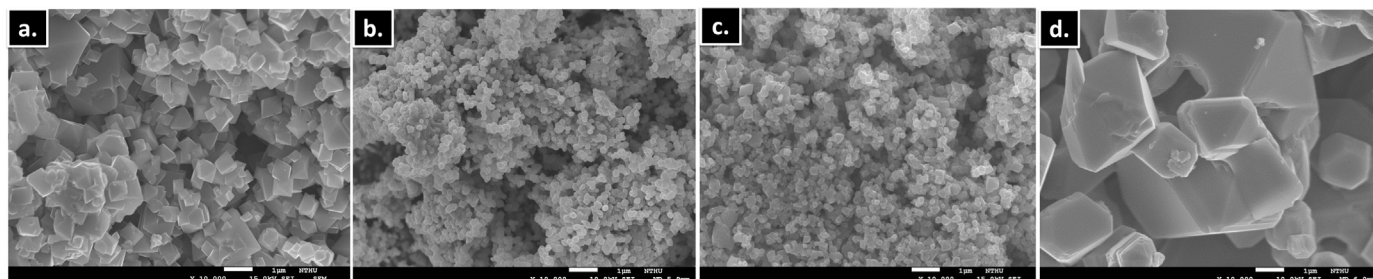


Fig. 2. FE-SEM images of $\text{LiNi}_{1/2}\text{Mn}_{3/2}\text{O}_4$ powder synthesized with/without polymer pre-mediation: (a) pristine, (b) PAA, (c) PEG, and (d) PI.

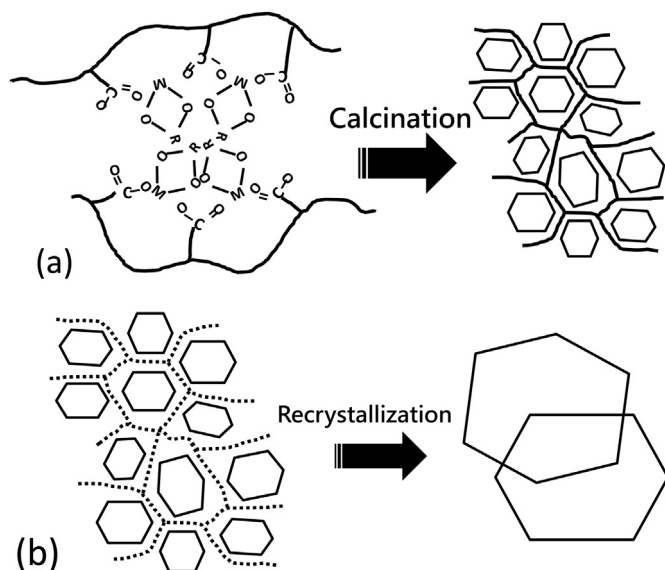


Fig. 3. Illustration of Li–Ni–Mn precursors (a) in the chelating process with the presence of PEG/PAA and (b) re-crystallization process with the presence of PI.

chelates in the presence of carbonyl polymer chains. The advantage of carbonyl functional groups is to bind metal ions together closer and shortens the diffusion paths for oxides to form. The process is based on the chemical adsorption of metal oxalates onto the polymer surface [18].

However, in the case of mediating of PI, the particle size of as-synthesized spinels was dramatically increased over 5–10 μm . Polyimide is an N-containing pyromellitic compound with an ultimately high decomposition temperature around 600 $^{\circ}\text{C}$, which is exactly overlapped with the formation temperature of spinel phases. Thus, thermal degradation of PI was suggested to induce the recrystallization of $\text{LiNi}_{1/2}\text{Mn}_{3/2}\text{O}_4$ at high temperature, resulting in crunchy-like morphologies as illustrated in Fig. 3(b). Table 1 lists basic properties of various functional polymers employed in this study.

The structural identification was examined by X-ray powder diffraction with Cu K α radiation. All samples possess well-crystallized spinel structure without any detectable impurities and contaminations as shown in Fig. 4. This demonstrates that the spinel phase of $\text{LiNi}_{1/2}\text{Mn}_{3/2}\text{O}_4$ can be retained even after dramatically morphology transformation by polymer pre-mediations. Spinel with the clearly octahedral shape and well-defined (111) facets is expected to perform an excellent electrochemical behavior, owing to the lowest internal stress during insertion/exertion of Li^+ [19].

In electrochemical tests, correlations among particle sizes, cycling performances and temperature durability of $\text{LiNi}_{1/2}\text{Mn}_{3/2}\text{O}_4$ cathode material are comprehensively investigated. Three samples with different particle sizes: sub-micro (pristine), nanometer (pre-

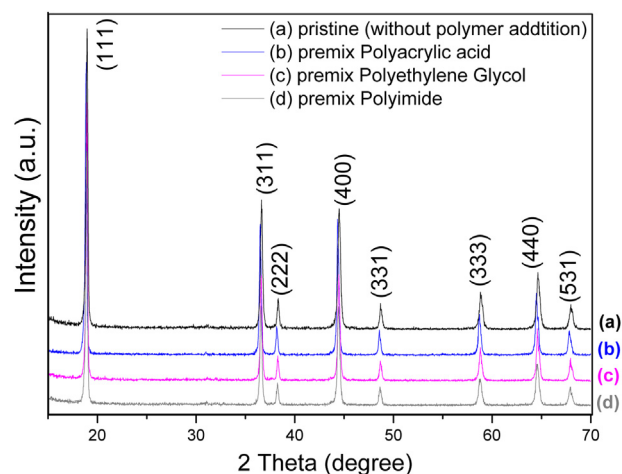


Fig. 4. X-ray diffraction patterns of $\text{LiNi}_{1/2}\text{Mn}_{3/2}\text{O}_4$ powder synthesized with/without polymer pre-mediation: (a) pristine, (b) PAA, (c) PEG, and (d) PI.

mediating of PEG), and micrometer (pre-mediating of PI) were assembled and performances were tested at various temperatures. As shown in Fig. 5(a), nano-sized particles delivered a higher discharge capacity about 122 mAh g^{-1} during cycled in 1C at room temperature. This is owing to a facilitated lithium intercalation in the smaller particle as compared to the large one at the same current input [20,21]. This impact can be much amplified while reducing the operation temperature during cycling. Fig. 5(b) exhibits the cycling performance of $\text{LiNi}_{1/2}\text{Mn}_{3/2}\text{O}_4$ with decrease of surrounding temperature (ie. 20, 10, 0, -10 , -20 $^{\circ}\text{C}$). The result clearly reveals that the use of nanometric particles can alleviate the severe capacity degradation of spinel materials, especially at an extreme low temperature such as -20 $^{\circ}\text{C}$. This is because the lithium ion diffusivity in electrolyte (10^{-5} – 10^{-6} $\text{cm}^2 \text{s}^{-1}$) is much larger than that in electrode (10^{-9} – 10^{-10} $\text{cm}^2 \text{s}^{-1}$) at an equivalent condition [22–24]. Therefore, a smaller particle with shortened lithium-ion diffusion path of electrode and a higher surface-contact area to the electrolyte leads to a better rate capability and capacity delivery, especially at low temperature.

The impedance spectroscopy was applied to investigate the charge state of $\text{LiNi}_{1/2}\text{Mn}_{3/2}\text{O}_4$ spinels as displayed in Fig. 6(a, b). When the cells are measured from ambient temperature to 10 $^{\circ}\text{C}$, no obvious difference in ohmic response was observed. However, as the temperature down to 0 $^{\circ}\text{C}$, a significant increasing in charge-transfer resistance (R_{ct}) was derived in the sub-micro particle with respect to nano-sized one. These evidences that a bigger particle encounters higher impedances during lithium de-intercalation as temperature down to 0 $^{\circ}\text{C}$ or lower. For detailed studies, charge–discharge curves were also plotted to examine the re-dox behaviors of $\text{LiNi}_{1/2}\text{Mn}_{3/2}\text{O}_4$ spinels as shown in Fig. 7(a, b). The voltage polarization of sub-micro particles increased more rapidly as compared with nano-sized one while temperature decreases. This indicates that a higher energy needs to overcome for bigger particles from lithium ion to migrate between electrode and electrolyte. The voltage interval of spinel samples between charge and discharge is recorded in Table 2.

For the feasibility of commercialization, the research progress in lithium ion battery must focus on long-term cycling stabilities of cathode materials [25–27]. Unfortunately, manganese-type spinels suffer from significant capacity decay at prolonged cycles due to the seriously corrosion in the acidic electrolyte, especially at elevated temperatures. The corrosion process causes some Mn^{2+} ions dissolved in non-aqueous electrolyte and leads to the irreversible capacity fading.

Table 1

Lists of molar weight and degradation temperature of various polymers used in this study.

Type of polymers	Molecular weight (g mol^{-1})	Solvent	Degradation temperature ($^{\circ}\text{C}$)
Polyacrylic Acid (PAA)	2200	H_2O	350–450
Polyethylene Glycol (PEG)	6000	H_2O	300–400
Polyimide (PI, Upilex-type)	10000–20000	NMP	600–700

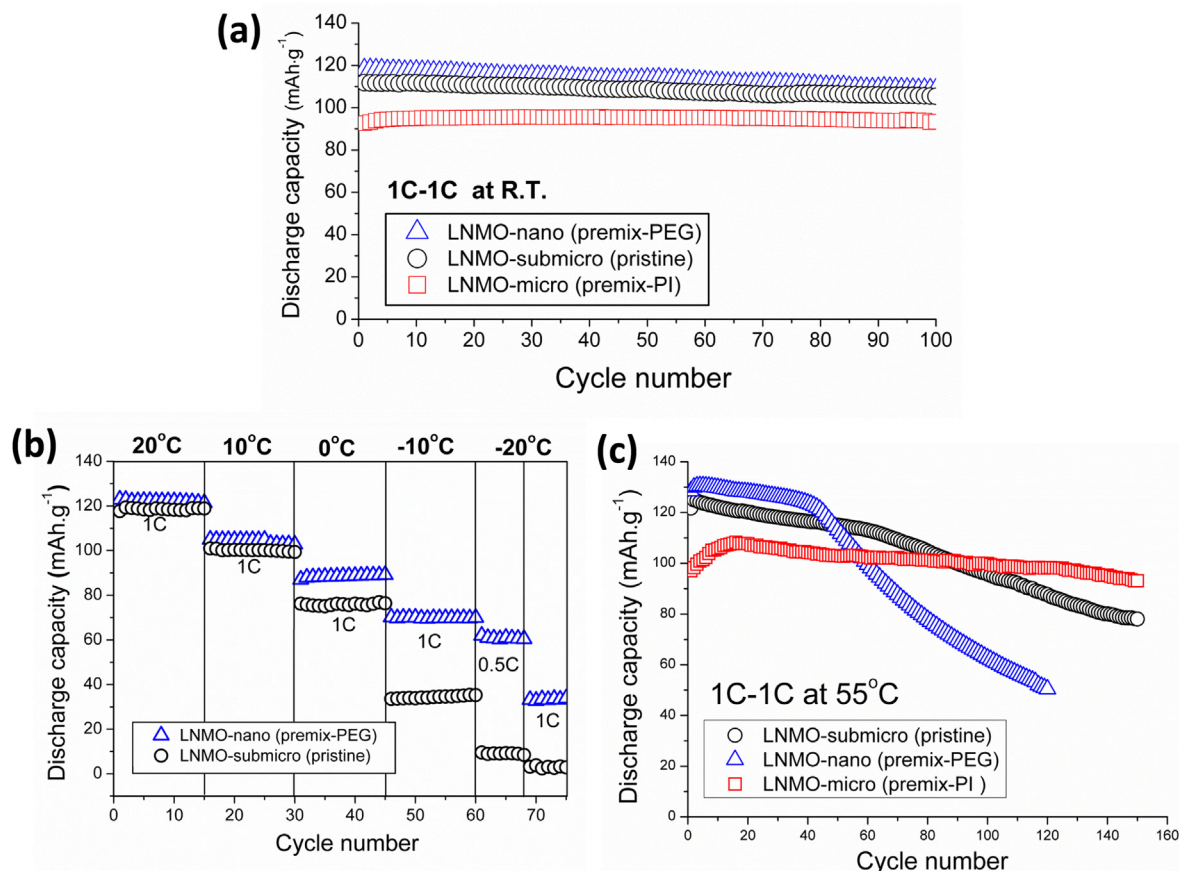


Fig. 5. Cycling performances of spinel $\text{LiNi}_{1/2}\text{Mn}_{3/2}\text{O}_4$ cathodes at (a) room temperature (b) reduced temperature from 20 to -20°C and (c) high temperature of 55°C .

Fig. 5(c) displays the cycling performance of $\text{LiNi}_{1/2}\text{Mn}_{3/2}\text{O}_4$ samples at 55°C . A severe capacity fading was observed in nano-sized particles right after 50 cycles, suggesting the irreversible structural destruction by numerous Mn ion dissolutions. On the other hand, good cycleability was maintained in micro-sized particle even after 100 cycles at 55°C . This result manifests that the severe capacity decay of $\text{LiNi}_{1/2}\text{Mn}_{3/2}\text{O}_4$ spinel can be relatively suppressed via magnifying the particle size of active materials, which is greatly attributed to the inhibition of surface contact between active material and electrolyte, retarding the rate of Mn ion dissolutions. It reveals that the appropriate particle size associated with $\text{LiNi}_{1/2}\text{Mn}_{3/2}\text{O}_4$ spinel via striking the balance between the fast intercalation and accelerated corruptions.

4. Conclusions

The use of polymer-mediating process in fabrication of high-voltage spinel cathode material was successfully demonstrated. The single phase $\text{LiNi}_{1/2}\text{Mn}_{3/2}\text{O}_4$ with various particle sizes was accomplished via changing the type of polymer additives. The long chain carbonyl polymer, such as PEG and PAA, favors the formation of nanometric powders. On the other hands, the mediation of PI prefers to generate large particle size. The thermal interference is speculated to associate with the coarsening of spinel powders. Electrochemical result shows good reversible capacity of as-synthesized spinels ranging from 100 to 120 mAh.g⁻¹ at room temperature. Nanometric spinels delivered a slightly higher capacitance and excellent rate

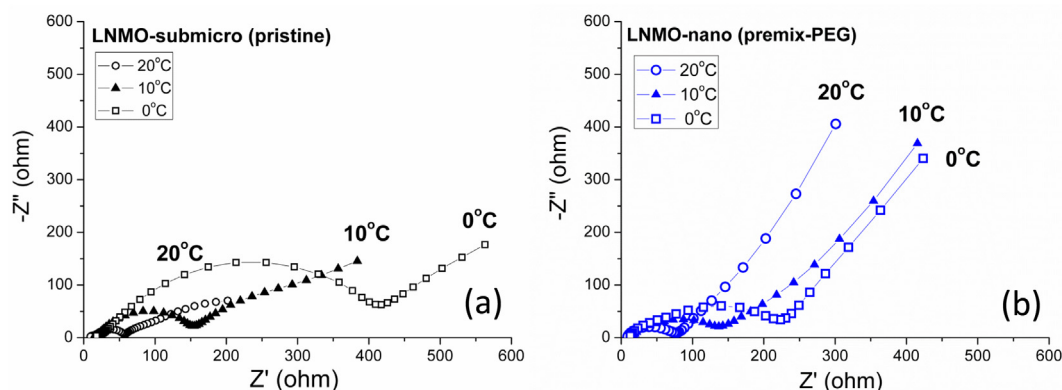


Fig. 6. Impedance spectroscopy of spinel $\text{LiNi}_{1/2}\text{Mn}_{3/2}\text{O}_4$ cathodes with (a) submicro and (b) nano-sizes as temperatures decreased from 20 to -20°C .

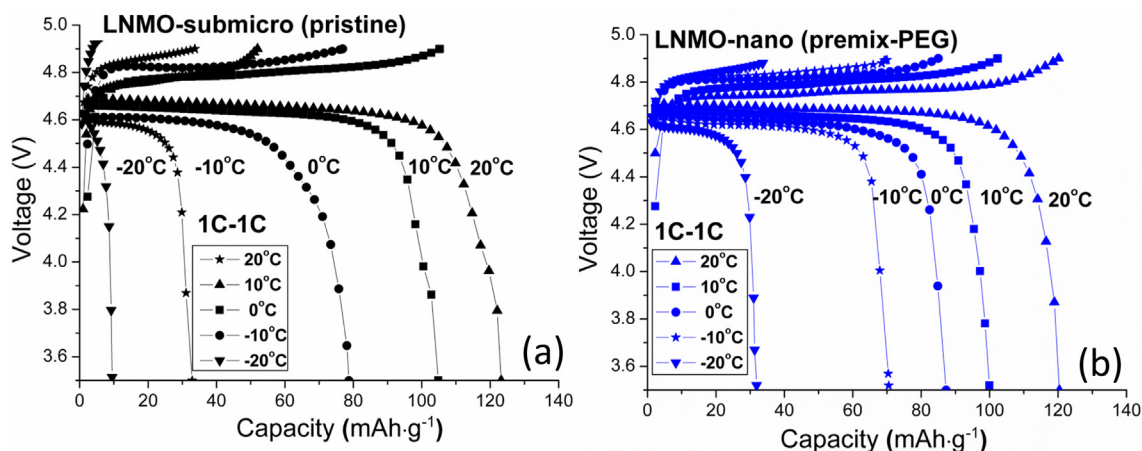


Fig. 7. Charge–discharge plot of spinel $\text{LiNi}_{1/2}\text{Mn}_{3/2}\text{O}_4$ cathodes with (a) submicro and (b) nano-sizes as temperatures decreased from 20 to -20°C .

Table 2

Voltage potential measurement of spinel $\text{LiNi}_{0.5}\text{Mn}_{1.5}\text{O}_4$ cathodes with different particle sizes.

ΔV (volts)	20 °C	10 °C	0 °C	−10 °C	−20 °C
Submicro	0.12	0.175	0.255	0.32	0.44
Nano	0.1	0.145	0.18	0.225	0.31

capability at reduced temperature, yet a poor cycleability at high temperature. The enhanced capacity stability was achieved in micro-sized $\text{LiNi}_{1/2}\text{Mn}_{3/2}\text{O}_4$ spinel during cycled at 55°C . It reveals that the size of spinels contributes to the enhancement of the reliability by varying the specific surface-area, and by enhancing the resistance to electrochemical failure, especially at elevated temperature. As the consequence, through synergistically considering electrochemical performance and temperatures durability, the prominent particle size could be therefore derived.

Acknowledgment

The author acknowledges financial support from Industrial Technology Research Institute (ITRI) of Taiwan (102A0127J4).

Appendix A. Supplementary data

Supplementary data related to this article can be found at <http://dx.doi.org/10.1016/j.jpowsour.2014.03.089>.

References

- [1] Y.P. Fu, Y.H. Su, C.H. Lin, S.H. Wu, J. Mater. Sci. 41 (2006) 1157.
- [2] Y.C. Sun, Z.X. Wang, X.J. Huang, L.Q. Chen, J. Power Sources 132 (2004) 161.
- [3] Y.K. Sun, K.J. Hong, J. Prakash, K. Amine, Electrochem. Commun. 4 (2002) 344.
- [4] J. Molenda, J. Marzec, K. Świerczek, D. Pałubiak, W. Ojczyk, M. Ziemiński, Solid State Ionics 175 (2004) 297.
- [5] Y. Ein Eli, J.T. Vaughey, M.M. Thackeray, S. Mukerjee, X.Q. Yang, J. McBreen, J. Electrochem. Soc. 146 (3) (1999) 908.
- [6] H.S. Fang, Z.X. Wang, X.H. Li, H.J. Guo, W.J. Peng, J. Power Sources 153 (2006) 174.
- [7] Q. Zhong, A. Bonakdarpour, M. Zhong, Y. Gao, J.R. Dahn, J. Electrochem. Soc. 144 (1997) 205.
- [8] Y. Idemoto, H. Sekine, K. Ui, N. Koura, Solid State Ionics 176 (2005) 299.
- [9] S.T. Myung, S. Komaba, N. Kumagai, H. Yashiro, H.T. Chung, T.H. Cho, Electrochim. Acta 47 (2002) 2543.
- [10] Y.S. Lee, Y.K. Sun, S. Ota, T. Miyashita, M. Yoshio, Electrochem. Commun. 4 (2002) 989.
- [11] J.H. Kim, S.T. Myung, Y.K. Sun, Electrochim. Acta 49 (2004) 219.
- [12] S.H. Park, S.W. Oh, S.T. Myung, Y.K. Sun, Electrochim. Solid State Lett. 7 (2004) A451.
- [13] D. Liu, J. Han, J.B. Goodenough, J. Power Sources 195 (2010) 2918.
- [14] U. S. Pat. 3(330) (1967) 697.
- [15] W. Vu, C.C. Forrington, F. Chapur, B. Dunn, J. Electrochem. Soc. 143 (3) (1996) 879.
- [16] Y.C. Jin, J.G. Duh, Mater. Lett. 93 (2013) 77.
- [17] J.C. Arrebola, A. Caballero, L. Hernán, J. Morales, Eur. J. Inorg. Chem. (2008) 3295.
- [18] J. Huang, N. Matsunaga, K. Shimanoe, N. Yamazoe, T. Kunitake, Chem. Mater. 17 (2005) 3513.
- [19] Lithium Ion Rechargeable Batteries, Wiley Vch, Kazunori Ozawa, 2009, pp. 11–24.
- [20] A.S. Aricò, P.G. Bruce, B. Scrosati, J.M. Tarascon, W.A. Schalkwijk, Nat. Mater. 4 (2005) 366.
- [21] Y. Mosqueda, E. Pérez-Cappe, P. Aranda, E. Ruiz-Hitzky, Eur. J. Inorg. Chem. 13 (2005) 2698.
- [22] K. Tasaki, A. Goldberg, J.J. Lian, M. Walker, A. Timmons, S.J. Harris, J. Electrochem. Soc. 156 (12) (2009) A1019.
- [23] M. Park, X. Zhang, M. Chung, G.B. Less, A.M. Sastry, J. Power Sources 195 (24) (2010) 7904.
- [24] L.O. Valøen, J.N. Reimers, J. Electrochem. Soc. 152 (5) (2005) A882.
- [25] J.C. Arrebola, A. Caballero, L. Hernán, J. Morales, J. Power Sources 195 (2010) 4278.
- [26] T. Noguchi, I. Yamazaki, T. Numata, M. Shirakata, J. Power Sources 174 (2007) 359.
- [27] K. Amine, J. Liu, S. Kang, I. Belharouak, Y. Hyung, D. Vissers, G. Henriksen, J. Power Sources 129 (2004) 14.